We are IntechOpen,
the world's leading publisher of
Open Access books
Built by scientists, for scientists

6,900
Open access books available

186,000
International authors and editors

200M
Downloads

154
Countries delivered to

Our authors are among the

TOP 1%
most cited scientists

12.2%
Contributors from top 500 universities

WEB OF SCIENCE™

Selection of our books indexed in the Book Citation Index
in Web of Science™ Core Collection (BKCI)

Interested in publishing with us?
Contact book.department@intechopen.com

Numbers displayed above are based on latest data collected.
For more information visit www.intechopen.com

A New Laser Scanning System for Computed Radiography

Qibo Feng, Meng Zheng, Shuangyun Shao and Zhan Gao
School of science, Beijing Jiaotong University, Beijing 100044
P. R. China

1. Introduction

X-ray inspection is widely used in aviation, aerospace, weapons, nuclear energy, automobile and other fields for non-destructive testing and non-destructive evaluation. It plays an important role in engineering quality supervision and quality control, and it has become a basic technology in industry and high-tech industry.

With the strength of visuality, high sensitivity and high resolution, X-ray screen-film radiography is widely used in industrial non-destructive testing, medical imaging and other fields. However, it has some disadvantages of low efficiency and films being not reusable. Due to this, there have been some new methods of digital imaging for radiographic inspection such as the analog imaging based on image intensifier, the large array detector imaging based on Thin Film Transistor (TFT), and the computed radiography (CR) imaging based on the photo-stimulated luminescence (PSL). As the imaging plate of a CR system has some advantages of large dynamic range, erasibleness, high sensitivity, high spatial resolution, flexibility, etc. It has become a key research field (Brandt, 1993; Cowen et al., 2007; Dragusin et al., 2006; Satoshi et al., 1999; Schaetzing et al., 2002). Some commercial CR systems, especially for medical imaging, have also emerged.

With higher production standards for long-distance oil and gas pipeline systems, X-ray inspection of pipe ends and patching has become a key means for inspecting harmful defects in major domestic and international long-distance pipelines in order to guarantee their quality. Having shared the merits of industrial film radiography of large ray dosage absorption, flexibility, and higher spatial resolution, CR systems also enjoy new edges such as digital imaging, large image dynamic range and re-usable image plate, and it will play a key role in industry applications such as pipe quality testing and controlling. However, the high cost of CR systems has hindered their development in the field of industrial testing which is not so profitable. Therefore, to sharpen the competitive edge of CR systems in industrial testing, it is necessary not only to improve the inspection efficiency and image quality of the image plate, but also to significantly reduce the costs of CR systems.

Readout technology and equipment are the key technology and core part of CR systems and it also play a key role in the cost of the CR system. Theretofore, how to improve the resolution and scanning speed of readers and how to efficiently collect weak fluorescent signals in a simpler way and lower cost have been a focus for studies in this field.

2. The point-scanning methods for CR systems

A CR system mainly consists of three parts: information recording, completed by the imaging plate; image scanning and reading, done by the CR scanner; image processing and storing, undertaken by the computer and memory devices. Taking the industrial X-ray inspection of welding defects as an example, the specific work procedure of a CR system is shown in Fig.1.
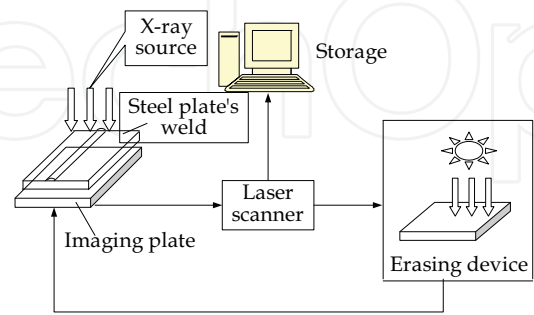

Fig. 1. CR system work flow

As shown in Fig.1, the CR system replace the conventional X-ray screen-film with a reusable imaging plate (IP) coated with a photo-stimulating storage phosphor, which retains latent image information when the IP is exposed to X-ray and the information of the X-ray energy is stored. Then the IP will be put through the laser scanner that reads and digitizes the image, and the image is stored in memory. When the laser scanner has collected all information on the IP, the IP will be taken to erasing device to clear the recorded information so that it can be re-used next time.
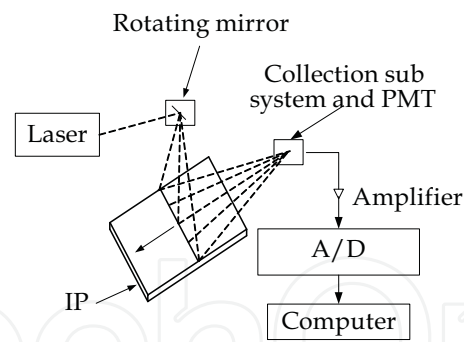

Fig. 2. Readout procedure of IP

The CR scanner is the core part of the CR system. Currently, there are mainly two kinds of scanning methods that are point-scanning and line-scanning. The procedure of the point-scanning and imaging is shown in Fig. 2. As the IP is exposed, the latent image is retained on fluorescent substances. Through the optical scanner such as a rotating mirror, the laser beam coming from the laser source is projected toward the IP to form a line scanning. As the IP moves along the direction of vertical scanning beam, a column scanning is formed. The weak luminescence signal excited by the laser beam on the IP will be gathered by a photomultiplier tube through a luminescence optical collection device, and the signal from the photomultiplier tube will be amplified and put into a computer for processing through the A/D converter. Finally, the intensity value on one point of the IP can be obtained, and the whole high-quality digital images of the IP are produced through point by point scanning.

Compared with the line-scanning, the point-scanning has the advantages of simple configurations, low requirements for the laser source and the photo-detector and low cost, it has been widely adopted in CR systems. Currently, there still are different kinds of optical point-scanning in designing the CR scanner, which commonly works in the following ways:

(1) **Scanning Using a Rotary Polyhedron and a $F\theta$ Lens**. As shown in Fig. 3(Shan B Zh et al., 2005), in the scanning optical path of the IP, a rotary polyhedron is used for the scanning and a $F\theta$ lens is used for focusing the laser beam. The use of the $F\theta$ lens is to make sure that scanning spot maintain a linear movement on the IP in order to eliminate the distortion of scanning. However, the rotary polyhedron prism scanning will inevitably cause the discontinuity of scanning beams between two adjacent faces of the polyhedron prism, and there is a signal vacuum during the discontinuity time. Meanwhile, the rotary polyhedron has also caused some problems such as the sway and displacement error of the rotating shaft, the division error of the rotating mirror and the tilt error of reflector, all these errors directly influence the quality of the scanning and they are difficult to get rid of. In addition, it is difficult to for the laser beam to keep a linear movement by using a $F\theta$ lens, and using a $F\theta$ lens makes the CR system much more complicated and costs more money.
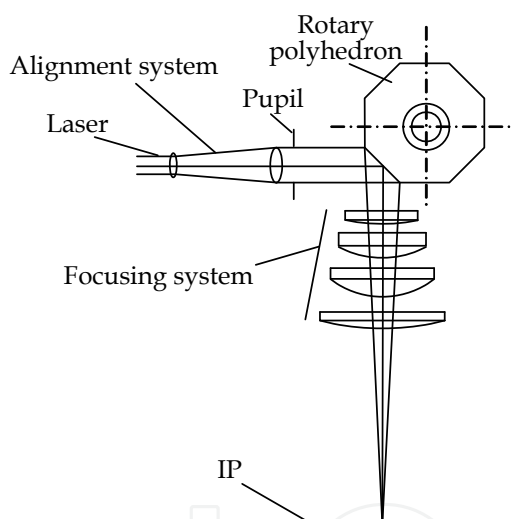

Fig. 3. Scanning with a $F\theta$ Lens

(2) **Scanning Using a Pentagonal Prism and a $F\theta$ Lens.** As shown in Fig. 4(Zhang J P et al., 2008), two pentagonal prisms are used for scanning the laser beam, and a $F\theta$ lens is used for focusing the laser beam. The collimated laser beam is first scanned by rotating the pentagonal prism, and then the laser beam is projected to the $F\theta$ lens, through which the laser beam is focused to a point on the IP that is in the focal plane of the $F\theta$ lens, a line scanning is formed by rotating the pentagonal prism, and whole digital image of the IP can be obtained when the IP move along the direction that is perpendicular to the scanning line. Two pentagonal prisms are used to enhance the efficiency of the scanning and to reduce the scanning time. This type of point-scanning can overcome the problem of discontinuity as shown in Fig.3, however, it has the same disadvantage of the complicated optical system and high cost as a complicated $F\theta$ lens is needed.
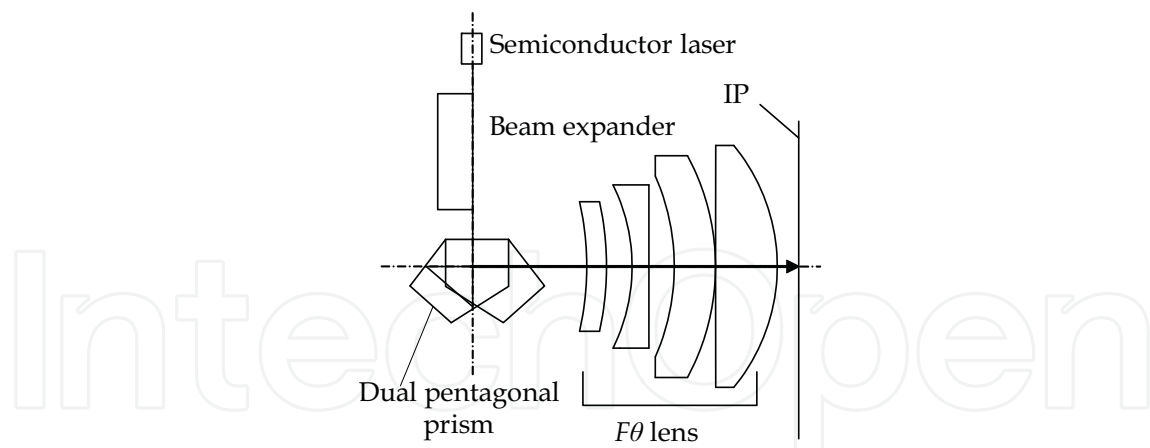
Fig. 4. Scanning with $F\theta$ and pentagonal prism

(3) **Scanning Using a Single Piece of Tilting Reflecting Mirror**. As shown in Fig.5 (Chen H Q, 2003), an objective lens and a single mirror are used to focus the laser beam to a point on the IP. Theoretically, a line scanning can be formed if the mirror is rotated around the axis that is also the axis of both the objective lens and the circular IP. It can be seen that the incident light beam occupies the whole surface of the mirror during the scanning and only one piece of mirror is required for the scanning. There is no transition of beam between mirrors and consequently no discontinuity during the laser beam scanning. Therefore, the receiving field is arc-shaped, the focused laser beam moves at a constant speed in the circular IP and a linear scanning can be gotten. This type of point-scanning has the advantages of a simpler optical system and lower cost of the scanning system; it has been adopted by some companies in their commercial CR systems. However, as there is inevitably a tilt of θ during the rotating of the mirror, the direction of the laser beam reflected by the rotating mirror will change 2θ, causing a position change of the focused laser beam point in the IP and worsening the quality of the image from the IP.
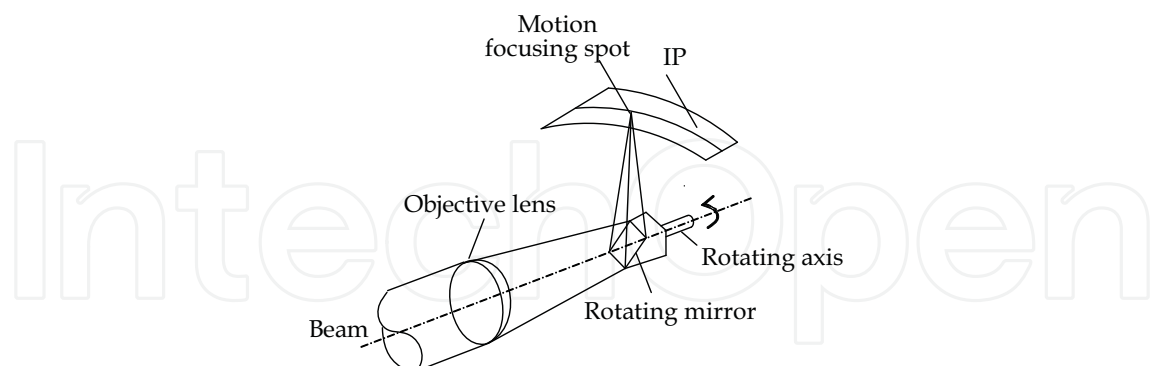
Fig. 5. Scanning with a single mirror

(4) **Scanning Using a Pyramid-shaped Rotating Mirror.** A pyramid-shaped multi-faceted prism is an equilateral prism, the surface of which tilts to form an angle with the rotating axis, placing itself under the full coverage of the beam, as shown in Fig.6 (Chen H Q, 2003). The major characteristic of the scanning with such a pyramid-shaped rotating mirror is that in order to make sure that the beam spot on the arc-shaped orbit for focusing moves with a uniform angular velocity, the focus of objective lens must be designed to be located on the rotation axis of the rotating mirror.
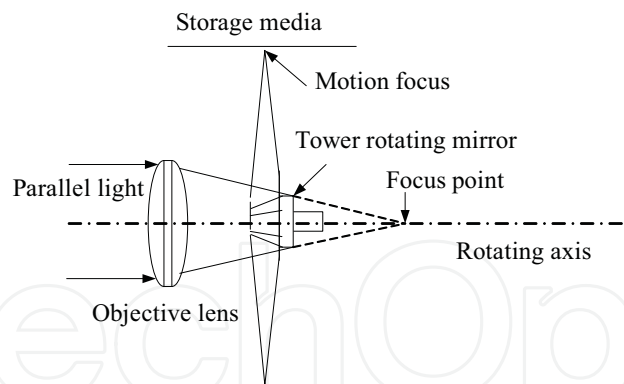
Fig. 6. Scanning by a pyramid-shaped mirror

In order to get stable scanning region, that is to say to eliminate scanning intermittence as much as possible, there must be at least two adjacent prism planes that are fully lightened in the effective scanning sector. The shortcoming of this kind of point-scanning is that it is difficult to manufacture a pyramid-shaped mirror, moreover, there will be inevitably a tilt of θ during the rotating of the mirror, and this will influence the quality of the image from the IP mentioned above in Fig.5. With the mirror plane inclining towards the axis, high-speed rotation will impose an uneven dynamic stress on the prism, which will in turn cause the shape of the prism to change.

In all four-kinds of point-scanning optical methods of the CR systems just mentioned above, a special separate optical collection system is needed in order to gather the weak fluorescence signals excited by the scanning laser beam.

In summary, the current point- scanning optical systems are mainly faced with the following problems: (1) Polyhedron prism scanners will cause the discontinuity of scanning beams, resulting discontinuity in information transmission; (2) The $F\theta$ lens as focusing device would bloat the overall structure of the system and result a complicated and costly optical scanning system; (3) The scanning optical system and the luminescence collection optical system are usually separated from each other, which calls for the designing and manufacturing of a separate luminescence collection optical system, resulting in a more complex optical system of CR systems.
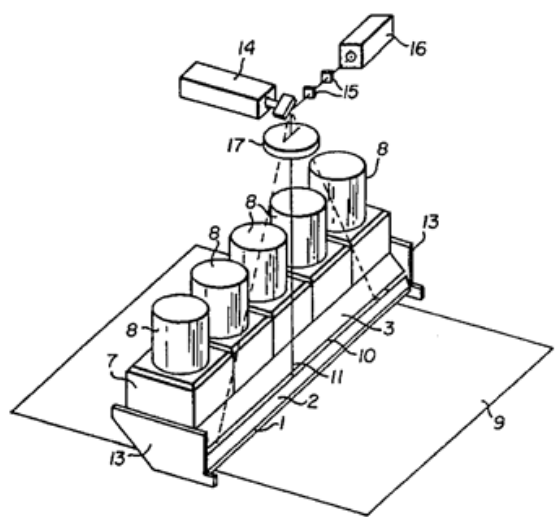

Fig. 7. Optical system of a CR scanner

A laser scanning system for computed radiography is shown in Fig.7 (Brandt et al., 1996). After being put through the beam expander 15, the laser beam emitted from a laser source 16 is turned into parallel light, and it is reflected by the laser beam scanner 14 and is focused on the IP 9 by the *Fθ* lens 17. The luminescent are simulated by the scanning beam 11 and gathered by the special collection optical system, which uses the plane mirrors and 1,2,3,13 stands for the four pieces of these plane mirrors, and then the luminescent are sent to the PMT 8 for amplifying and further processing. The stray light can be removed by using a filter 7.

3. The new laser scanning system for CR

3.1 Principles of scanning and imaging

To overcome these three problems of the existing CR scanning systems mentioned above, a new laser scanning optical system has been designed, as shown in Fig.8. After being put through the filter and the beam expander, the laser beam emitted from a laser source is turned into parallel light, which will go through a dichroic mirror and is subsequently reflected by a pentagonal prism and is then focused by a scanning objective lens onto the IP. Thus luminescent signals are produced by the simulation of phosphor, and photo-stimulated luminescence becomes parallel light after being collected by the scanning objective lens. Having gone through the pentagonal prism and been reflected totally by the dichroic mirror, the parallel light will be focused by the condenser, filtered by a filter to eliminate the stray light, and then sent into the photomultiplier tube, where it will go through A/D converter and be transmitted into the computer to acquire the luminescence gray value.

As shown in Fig.8, the pentagonal prism and the doublet objective lens are used to form a scanning arm for both stimulating and collecting luminescence on the IP. Only a dichroic mirror is adopted to separate the laser beam and the photo-stimulated luminescence, which simplifies the optical system. The dichroic mirror can transmit almost all laser beams and reflect all the luminescence, thus improving the luminescence collection efficiency.

While at work, the scanning arm is driven to rotate at a high-speed by the scanning motor to start a horizontal scan of the IP; the plate feeding structure is pulsed by the step motor forward to feed the IP vertically, thus scanning the whole IP point by point can be finished and the digitized image of the IP can be obtained.
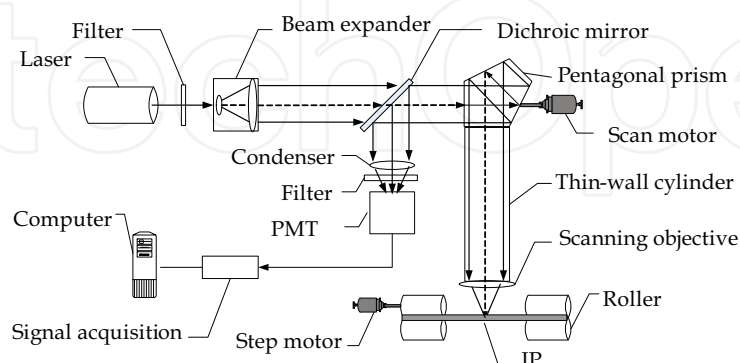

Fig. 8. Principle diagram of the CR scanner

To realize the rotation scanning, the IP has to be placed in the shape of a semi-circular arc and the circle central axis of the scaning arm shaft should coincide with the axis of the semicircular arc.

The configuration of the scanning optical system is shown in Fig.9. The advantages of such a scanning system is as follows: (1) The scanning optical system can guarantee that scanning laser beam is projected always vertically onto the IP and the focused spot of the laser beam on the arc keeps a continuous linear movement, there is no needs of using a $F\theta$ lens, resulting in a simpler and a lower price optical scanning system; (2) No need to design and manufacture a separate collection optical system as the scanning arm also can be used to collect the photo-stimulated luminescence, which further simplifies the scanning system.
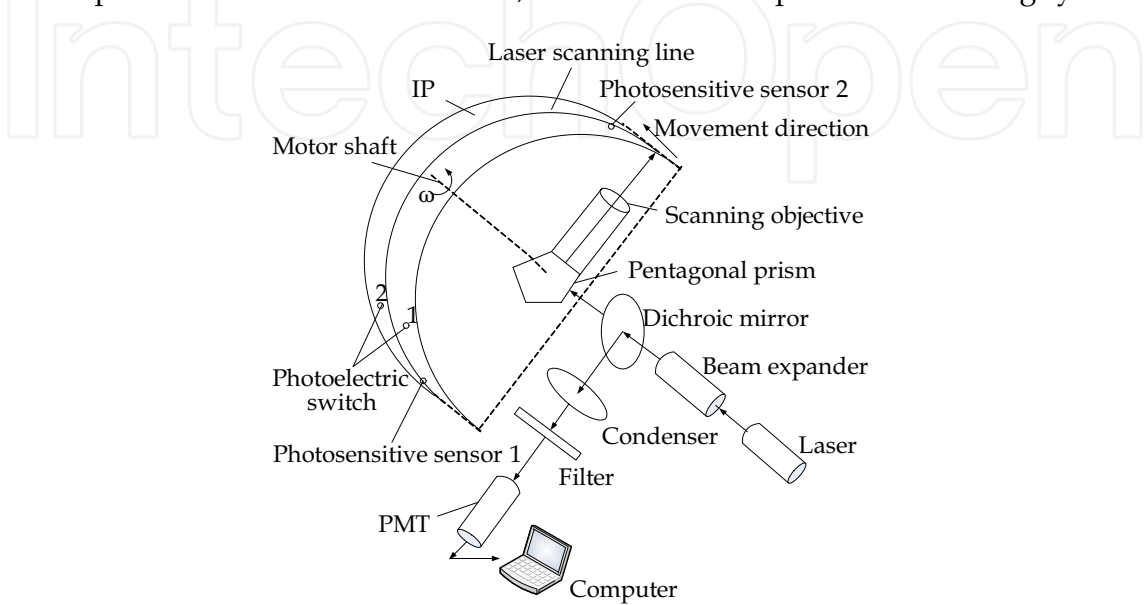

Fig. 9. Structure diagram of the CR scanner

3.2 Selections of key components
The laser source, the laser scanning objective lens and other components are quite vital to the performance of the scanning system. The following is a brief description of the selection strategy of these major components.
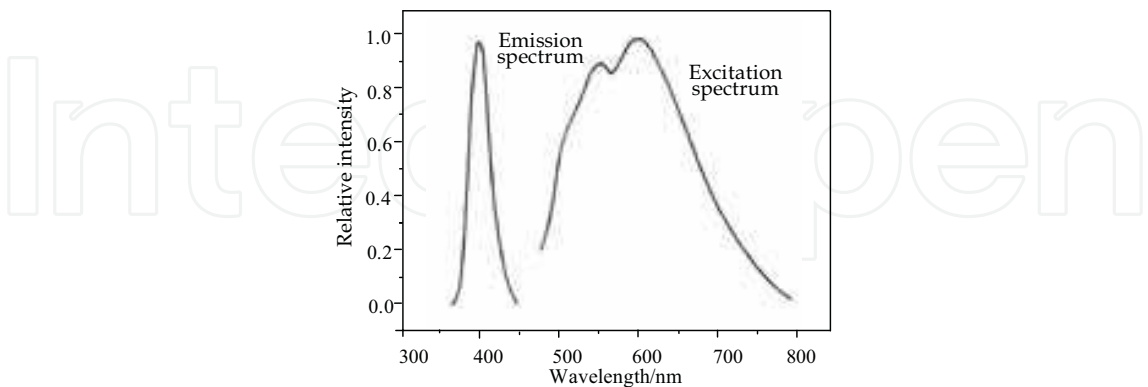

Fig. 10. Emission and excitation spectrum

(a) Laser

The emission spectrum and excitation spectrum curves of the IP are shown in Fig.10 (Zhou X L et al., 1993). The IP luminescence in this system has an emission peak wavelength of 390nm with its bandwidth of 20nm. The selected excitation laser beam has a wavelength of

638nm with its beam diameter about 0.8mm. To improve the quality of the laser spot, a single-mode coupled laser diode module has been adopted.

Within a certain range, the intensity of the luminescence stimulated on the IP is proportionate to both the X-ray energy stored in the IP and the exciting beam intensity.
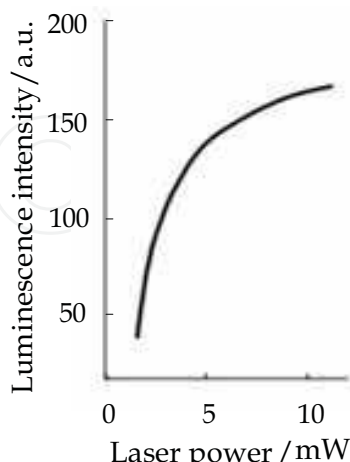

Fig. 11. Relationship between excitation flight intensity and laser power

Although excessively strong laser excitation beam can release more trapped electrons, the increased depth of the laser in the phosphor layer will enhance the excited luminescence diffusion and lower the probability of the stimulated luminescence to escape from the IP, resulting in lower collection efficiency. The relationship between the excited luminescence intensity and the power of the laser beam is shown in Fig.11 (Zhou X L et al., 1993), and it can be seen that a 10mw laser source is a good choice.

(b) Scan Lens

The scanning objective lens is an important component. For the excitation optical system, it must have a relatively small lens aberration to form a smaller laser scanning spot and to get a high spatial resolution; As far as the luminescence collection is concerned, the objective lens must have a greater numerical aperture in order to improve luminescence collection efficiency. The relationship between the excited luminescence on the IP and its emission direction can be expressed as follows

$$I = I_0 \cos\theta \tag{1}$$

Where I_0 is the luminescence intensity in the normal direction of the IP and θ the included angle with the normal direction.

The distribution of stimulated fluorescence from the IP is shown in Fig.12. The luminescence in the normal direction has the maximum intensity. With the increasing scattered angle, the stimulated fluorescence intensity is becoming lower. From Eq. (1), it can be gotten that $I = 0.866I_0$ if $\theta = 30°$. Across the scope of luminescence emission, a relatively strong luminescence can be collected within 30-degree solid angles formed by the launched luminescence with the normal direction. Therefore, the vertical excitation produces a concentrated energy distribution of the luminescence, and with an appropriate objective lens, relatively strong luminescence can be collected within the solid angle as shown in the Fig.12.
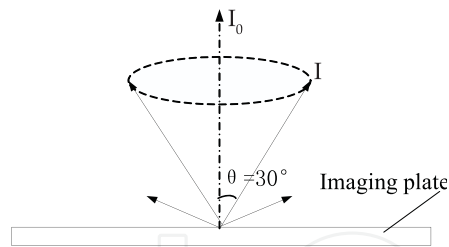
Fig. 12. Luminescence Distribution

A doublet lens is utilized as the scanning objective lens with the following parameters: the focal length $f = 25mm$, the back focal length $f_b = 15.6mm$, the diameter $\Phi = 25mm$, the effective aperture $CA = 22.5mm$ and thickness $t_c = 19mm$. For the luminescence gathering, the excited luminescence can fill the space of the lens aperture. For the laser beam excitation, as the laser beam has small diameter after collimation, it is approximately a paraxial beam, and the doublet lens can perfectly eliminate spherical aberration and coma. The calculated spot diagram is shown in Fig.13, which has a geometric aberration of a smaller size than the diameter of Airy disk and can meet the requirements for the scanning system.
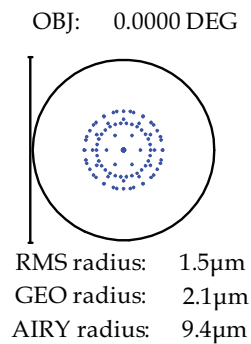
OBJ: 0.0000 DEG

RMS radius:	1.5µm
GEO radius:	2.1µm
AIRY radius:	9.4µm

Fig. 13. Spots diagram of the doublet lens

(c) Dichroic Mirror

As the luminescence excitation optical system and the collection optical system are common-path in this system, effective measures must be taken to separate the laser beam and the stimulated luminescence after the luminescence has been collected. To this end, a special dichroic mirror which can almost transmit the laser excitation beam with the wavelength of 638nm and reflect nearly all the luminescence with the wavelength of 390nm
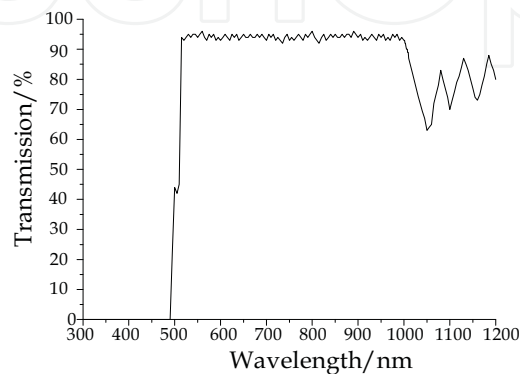
Fig. 14. Spectral curve of the dichroic mirror

was designed. Its properties are shown in Fig.14, and it can be seen that the dichroic mirror has the reflective band of 327-488nm with reflectance close to 100%, the transmission band of 515-850nm with the transmission rate of about 95%, thus contributing to the successful separation of the laser beam and the stimulated luminescence.

3.3 Computer signal acquisition and control

A control sub-system is mainly responsible for signal acquisition, motion control of the plate feeding sector, and synchronization between these two processes. The control scheme of the scanning system is shown in Fig.15.
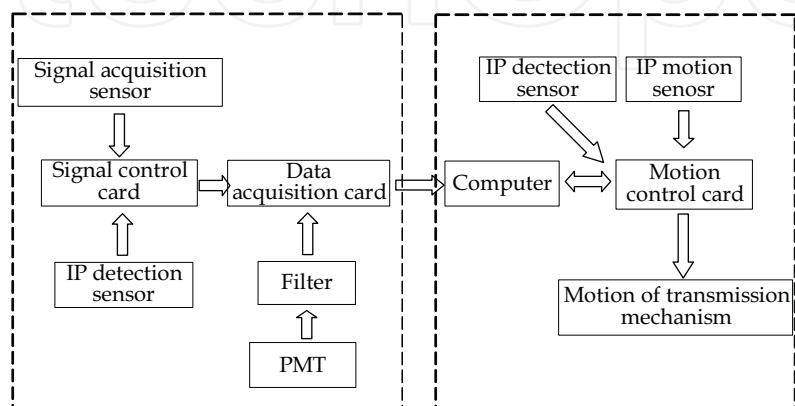

Fig. 15. Control scheme of the scanning system

As shown in Fig.9, the four sensors including two photoelectric switches and two photosensitive sensors are used to realize the synchronization and controlling of scanning, longitudinal movement of the IP and signal collection. Two photoelectric switches are longitudinally located on both sides of the laser scanning line, and can detect the entrance and exit of the IP through signals behind the NAND door. Two photosensitive sensors, which are triggered by the scanning laser beam, are located on the laser scanning line. When the scanning laser beam passes through the photosensitive sensor 1, the signal from the sensor 1 triggers the controlling circuit and the fluorescence signal is to be collected, at this time, the IP does not move; when the scanning laser beam passes through the photosensitive sensor 2, the circuit controls the IP move a step longitudinally and stop the fluorescence signal collection. Thus in the positive semi-circle of the scanning arm rotation path, the effective signal acquisition is under way. In the negative semi-circle, the stepper motor drives the IP to move one step forward. In this way, the scanning and imaging of the entire IP are completed.

The timing of overall control system is shown in Fig. 16.

When the scanner is powered up, the scanning motor and the laser start to work. When the scanning motor and the laser gains stability in their work, the IP, pushed by hand, has gone through the first optical switch, the IP detection output is a high level signal. Then stepper motor starts to work to move the IP quickly through a certain distance to reach the location of the scanning beam. Thereafter, the stepper motor regains normal speed with each step covering 50µm. The acquisition card goes into the normal acquisition state. When the scanning laser beam goes through photosensitive detector 1, signal acquisition is initiated. When it goes through the photosensitive detector 2, the stepper motor moves one step further. This process will be repeated until a complete image of the IP is gathered. When the
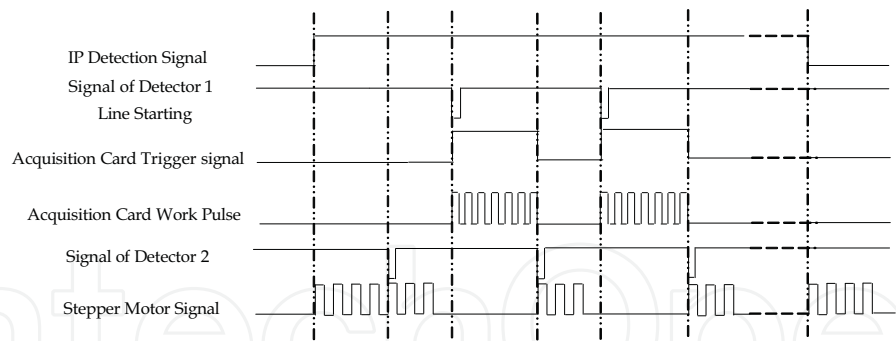
Fig. 16. Control system timing diagram

IP moves away from the two photoelectric switches, the IP detection signal output is at a low level and the acquisition card stops working. The stepper motor fast movement so that the IP can move fast out of the scanner and the whole scanning procedure is finished.

3.4 Mechanical system

On the one hand, the mechanical system should ensure the relative positions of the various components of the scanning system and their stability; on the other hand, it enables the rotation of the scanning arm and the movement of the plate driving mechanism as well as guarantees the accuracy of movement. The mechanical structure of the scanner designed according to these functions is shown in Fig.17. The photomultiplier tube lies below the excitation light path and its receiving window directly faces the luminescence emitting mouth of the dichroic mirror. While in the actual application, the photomultiplier tube is sealed in a tin box. The internal and external surfaces of the box are black anodized so that the photomultiplier tube remains in a shade environment. The scanning servo motor is fixed on a support, and the principal axis of the scanning motor is connected with the scanning arm and coincides with the optical axis of the scanning optical system.
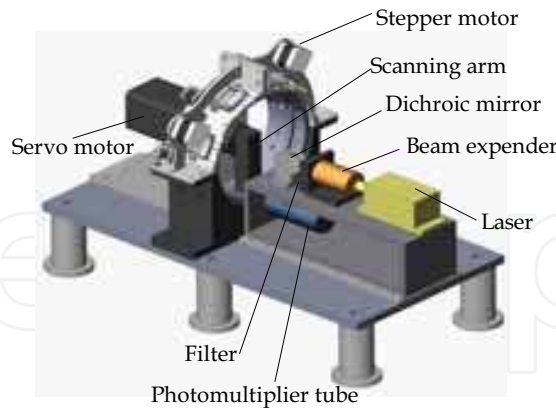

Fig. 17. Scheme diagram of the mechanical structure

3.5 Configuration of software

The software of the CR system is critical in keeping the system work properly. It is not only a program of human-computer interaction but also the center for controlling the system work and image acquisition and processing. It undertakes the tasks of deciding when to start work, displaying data that has been obtained after the IP is scanned, and image processing and weld defect identification.
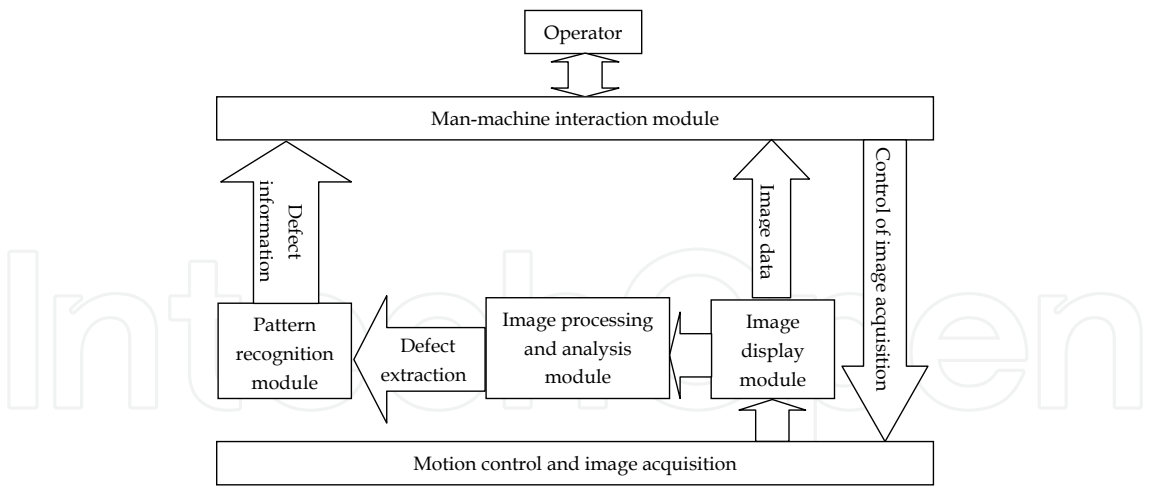
Fig. 18. Structure scheme of the software

As shown in Fig.18, the software of the scanner consists of four modules which are a human-machine interaction module that is responsible for defects identification and image gathering control; an image display module that is used for the conversion and storage of image data and the transmission of image data to the screen; an image processing and analysis module that is a systematic and modularized software for various image processing algorithms according to the inspection requirements, including a variety of basic image manipulation such as histogram transformation, image rotation, image reduction, basic filtering methods, and the geometric locations of the defects obtained through processing and analysis; a pattern recognition module that is used for the extraction of weld defects, marking, identification and classification.

The prototype of a computed radiography laser scanning system developed accordingly is shown in Fig.19.

Fig. 19. Prototype of the CR system

4. An analysis of the major factors influencing the performance of the system

The specifications that reflect the performance of the laser scanning systems mainly include the spatial resolution, the image stability and the speed of scanning and other parameters. The following is a brief analysis on these major factors so as to provide a basis for further improving such scanning systems.

4.1 The major factors affecting resolution of the system and related analysis

The spatial resolution of the CR image is related to properties of the IP, the laser spot size and the sampling frequency. In the scanner, the image is obtained by scanning the laser spot point by point on the IP, and the diameter of the laser spot is directly related to the quality of the image that has been read. Generally speaking, the smaller the diameter of the laser spot of the scanner is, the smaller the impact that it will have on the adjacent un-scanned IP latent image. And the image quality will be better and the resolution will be higher. Therefore, the laser spot size is an important factor that influences the spatial resolution of the system.
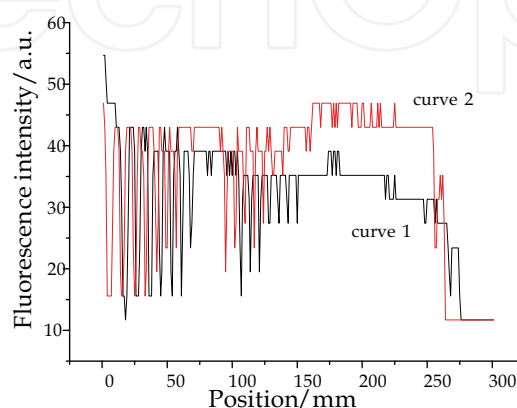

Fig. 20. Comparison with two laser spot size

The scanning curves by two different laser spot sizes are shown in Fig.20. In the experiment, 21 lead wires whose diameters are decreased in sequence are exposed to X-ray on the IP. The laser scanning system shown in Fig.19 was applied to scan the IP and a graph indicating the relationship between the luminescence intensity and its location was generated. In the graph, curve 1 represents the luminescence corresponding to the beam spot of 0.5mm in diameter and curve 2, the beam spot of 0.8mm diameter. The downward peaks show the wires that have been scanned. Curve 1 suggests that 16 wires can be distinguished, whereas curve 2 can only make it to 13. Therefore, the smaller the light spot size is, the higher the resolution will be.

The diameter of the laser spot should be as small as possible in order to obtain high spatial resolution. But the scanning arm deformation, the spherical aberration of the scanning objective lens, temperature deformation errors and installation errors will all cause the changes of the beam spot sizes of the laser beam on the IP, affecting the system's spatial resolution. Here is a simplified analysis:

(a) Scanning Arm Deformation

The mechanical structure of the scanning arm is shown in Fig.21. When the scanning arm begins to rotate at a high-speed, the centrifugal force will lead to the radial deformation of the scan arm, which will alter the distance between scanning objective lens and the IP, thus making the IP be not in the focus plane of the scanning objective lens and changing the diameter of the focusing spot.

A physical model of the scanning arm obtained by the three-dimensional mapping software is shown in Fig. 22. The scanning arm is made of the aluminium alloy 2024. With hexahedral element meshing, the result of the finite element analysis is that when the scanning arm rotates 4000 rounds per minute, the radial elongation is only 5μm, having little impact on the laser spot size and thus barely affecting spatial resolution of the scanning system.
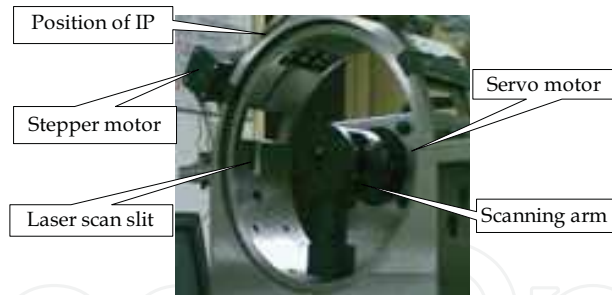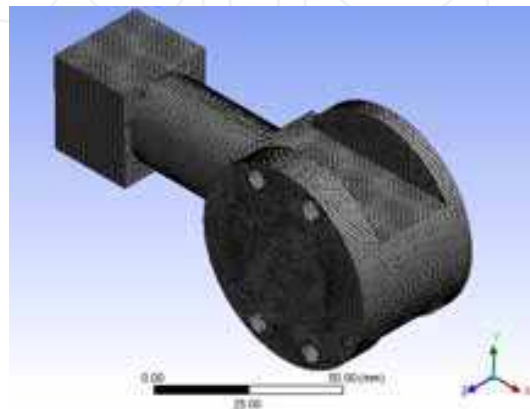
Fig. 21. Mechanical structure of the scanning arm

Fig. 22. Finite element mesh of scanning arm

(b) Spherical Aberration of the Scanning Objective Lens

The spherical aberration of the scanning objective lens will modify the beam waist in the image space, which means that the size of the focused spot changes and the spatial resolution of the system will reduce. In the laser scanning system, the selected laser source has following parameters: the incident laser wavelength $\lambda = 638nm$, beam waist radius $2\omega_0 = 2.4mm$. Since the image of this scanning system is mainly formed by axial laser beams, only the spherical aberration is considered here.

Theoretical derivation leads to the following formula expressing the relationship between the variant $\Delta\omega_0'$ representing the image space beam waist radius and the variation $\Delta R(z')$ representing the radius of curvature of the outgoing spherical wave (i.e., wave-front aberration)

$$\Delta\omega_0' = \frac{\pi^2\omega^5(z)}{\lambda^2}\left\{1 + [\frac{\pi\omega^2(z)}{\lambda}]^2[\frac{1}{R(z)} - \frac{1}{f'}]^2\right\}^{-3/2}[\frac{1}{R(z)} - \frac{1}{f'}]^3\Delta R(z') \tag{2}$$

Where $\omega(z)$ stands for the radius of the light spot that the incident beam projects on the lens, $R(z)$ for the radius of curvature of the incident spherical wave, and f' for the focal length of the lens.

The relationship between the wave-front aberration of the optical system and the longitudinal spherical aberration can be gotten by

$$OPD = -\frac{n'}{2}\int LA'du'^2 \tag{3}$$

Where n' is the image space refractive index, LA' the longitudinal spherical aberration and u' the image space aperture angle and the exit surface divergence angle in the laser transmission.

The spherical aberration is dominated by the third order spherical aberration in most optical systems. As far as the third order spherical aberration alone is concerned, the following formula will hold

$$\Delta R(z') = OPD = -\frac{1}{4}n'\sin u'^2(a_2y^2) = -\frac{1}{4}n'\sin u'^2 LA' = -\frac{1}{4}n'u'^2 LA' \tag{4}$$

Formula (2) minus formula (4) represents the relation between the variant $\Delta\omega_0'$ for the image space beam waist radius and the variant LA' for the spherical aberration of lens.

In the actual system, the distance from the incident light beam waist to the lens stands at $z = 200mm$. With the application of a commercial optical design software system, the spherical aberration of the doublet lens adopted by the system can be obtained. When formula (2) - formula (4) is applied, the wave-front aberration of lens can be obtained $OPD = 0.11\mu m$ and the variation of beam waist spot diameter is 0.44 ‰, which can be neglected.

It shows that the spherical aberration of the doublet lens utilized by the system is properly adjusted and has little impact on the size of focused laser beam spot and spatial resolution. However, if the scanning objective lens has a larger spherical aberration, it will result in an expanded diameter of the scanning laser spot and reduce the spatial resolution of the scanning system.

(c) Temperature Changes

In the most cases, the laser scanning system is used for the in-site applications, the temperatures of the environment are subjected to drastic changes. Since the scanner contains both optical and mechanical systems, changes in temperature will affect these systems and may eventually lead to enlarging the diameter of the laser spot at the IP, in which case the system's spatial resolution will reduce. However, through theoretical analysis, it can be discovered that in the temperature range from -10 °C to 50 °C, the system resolution is almost free from the impact of the environmental temperature.

(d) Installation Error

If there are some misalignments in adjusting the excitation optical system, especially in adjusting the laser source, as shown in Fig.23, the incident beam will not be perpendicular to the incidence surface of the pentagonal prism, in which case the axis of the scanning beam will not be perpendicular to the IP either. If there is an installation error in assembling the scanning arm, especially assembling the pentagonal prism, as shown in Fig.24, making the axis of the scanning beam be not perpendicular to the IP, the axis of the scanning beam will not be perpendicular to the IP either. In both cases, the size and shape of the scanning spot on the IP will change and the efficiency of luminescence collection will also be undermined.

The experimental results of the relationship between the incident angle of the scanning laser beam and the intensity of the luminescence collected after having excited IP is shown in Fig.25. It can be observed that when the incident angle enlarges gradually, the intensity of the luminescence collected will decrease and the collection efficiency will drop; when the axis of the scanning laser beam stimulates the IP perpendicularly, the luminescence intensity
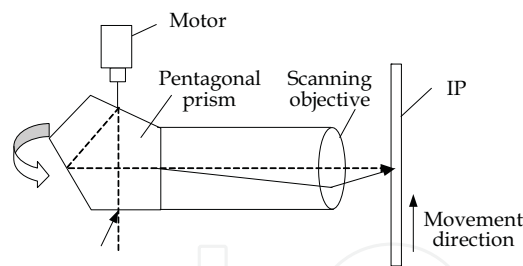
Fig. 23. The incident light be not perpendicular to incident plane of the pentagonal prism
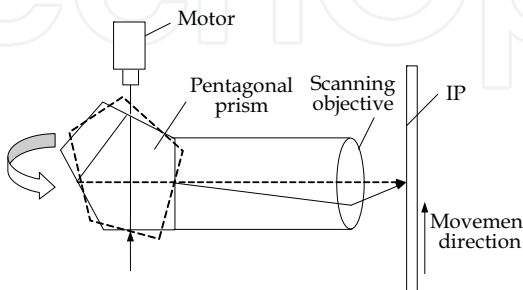

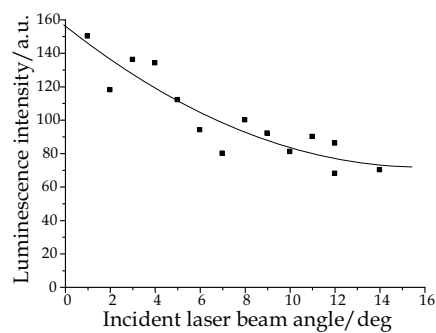Fig. 24. Pentagonal prism with installation error

Fig. 25. Relation between angle & luminescence intensity

is the highest and collection is the most efficient. Therefore, when assembling the system, the optical system should be carefully aligned so that the incident laser beam and the IP can be as perpendicular to each other as possible.

It is difficult to ensure that the shaft of the scanning motor and the spindle of the circular plate feeding sector completely be coaxial during the assembling process of the scanning system, and this deviation will cause the IP on the plate feeding sector to be away from the focal plane of the scanning objective lens to somewhere before or behind it, creating the IP positioning error, as shown in Fig.26. In theory, the IP should be at the focal plane of the scanning objective lens, as in such a condition the laser spot diameter is the smallest and the spatial resolution of the system is the highest; when the IP has a positioning error, the spot diameter will become larger and the system's spatial resolution will reduce.

Considering all the types of installation errors mentioned above, i.e., the laser misalignment, the pentagonal prism assembling error, the IP position error generated by the off-axis between the shaft of rotating parts and the spindle of the circular plate feeding body, the formula for the transmission of decentred Gaussian beams through the optical systems is derived (Abdul-Azeez et al., 1995; Palma, 1997), and the law governing the influence of

decentred Gaussian beams cases on the intensity of focusing light can be obtained. The transmission of decentred Gaussian beams through the focusing system is shown in Fig. 27.
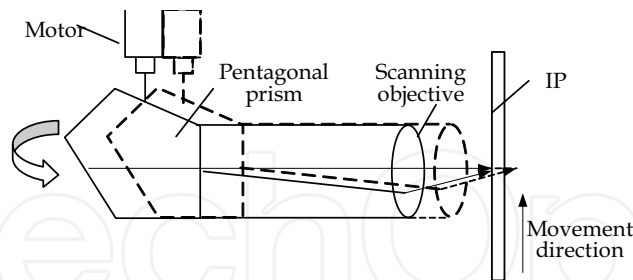

Fig. 26. Shaft of rotating parts and the principal axis of circular plate feeding sector being not coaxial
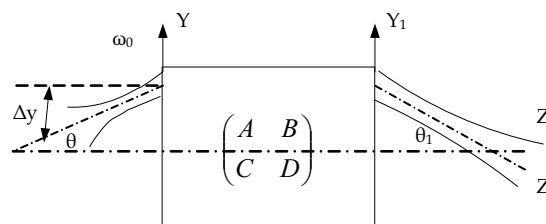

Fig. 27. Transmission of decentred Gaussian beams through the optical system

As shown in Fig.27, the input reference plane is at the waist of the incident beam and the output reference plane could be anywhere behind the objective lens. Z stands for the direction of the main axis of the objective lens, θ for the angle formed by the Gaussian beam and the axis Z, Δy for the displacement of the central ray of the entering light beam at the entering reference plane in the Y direction relative to the main axis of the optical system, ω_0 for the radius of the incident beam waist. To simplify the analysis, only one dimension is considered. The optical field distribution of the incident Gaussian beam at the plane of its waist is as follows

$$E_0(y_0,0) = \exp\left[-\frac{(y_0 - \Delta y)^2 \cos^2\theta}{\omega_0^2} \right]$$ (5)

Where y_0 stands for the coordinate value of the laser beam in the cross section. When the Gaussian beam goes through the optical system, its field distribution on the output reference surface can be known from the Collins formula

$$E_1(y_1,z) = \sqrt{\frac{ik}{2\pi B}} \int_{-\infty}^{+\infty} E_0(y_0,0)\exp\left[-\frac{ik}{2B}(Ay_0^2 - 2y_0 y_1 + Dy_1^2) \right] dy_0$$ (6)

Where λ is the wavelength, k the wave number, and A, B, C and D the transformation matrix elements for the optical system. The phase factor $\exp(-ikl)$ is omitted here.
Substituting Eq. (5) into Eq. (6) and applying integral Eq. (7)

$$\int_{-\infty}^{+\infty} \exp(-p^2 x^2 \pm qx)dx = \frac{\sqrt{\pi}}{p}\exp(\frac{q^2}{4p^2}) \ (p > 1)$$ (7)

The field distribution of the output reference plane can be expressed as

$$E_1(y_1,z) = \sqrt{\frac{ik}{2\pi B}} \cdot \exp\left(-\frac{ikDy_1^2}{2B}\right) \cdot \exp\left(-\frac{\Delta y^2 \cos^2\theta}{\omega_0^2}\right) \cdot \frac{\sqrt{\pi}}{p} \cdot \exp\left[-\frac{k^2(y_1-q)^2}{4B^2 p^2}\right] \quad (8)$$

Where $q = \dfrac{2i\Delta yB\cos^2\theta}{k\omega_0^2}$ and $p^2 = \dfrac{\cos^2\theta}{\omega_0^2} + \dfrac{ikA}{2B}$

The light intensity of Gaussian beam on the output reference plane can be written as

$$I_1(y_1,z) = E_1(y_1,z) \cdot E_1^*(y_1,z) \quad (9)$$

$E_1(y_1,z)$ can be obtained from Eq. (8), and $E_1^*(y_1,z)$ represents the conjugate of $E_1(y_1,z)$. Taking Eq. (8) into Eq. (9) with adjustment will lead to

$$I_1(y_1,z) = \sqrt{\frac{k^2}{4\pi^2 B^2}} \cdot \exp\left(-\frac{2\Delta y^2 \cos^2\theta}{\omega_0^2}\right) \cdot \frac{\pi}{\sqrt{\dfrac{\cos^4\theta}{\omega_0^4} + \dfrac{k^2 A^2}{4B^2}}} \cdot \exp\left(-\frac{k^2}{4B^2} \cdot \frac{q_1}{p_1}\right) \quad (10)$$

Where $q_1 = 2y_1^2\cos^2\theta - \dfrac{8\Delta y^2 B^2\cos^6\theta}{k^2\omega_0^4} - 4y_1\Delta yA\cos^2\theta$ and $p_1 = \dfrac{\cos^4\theta}{\omega_0^2} + \left(\dfrac{kA\omega_0}{2B}\right)^2$

Since the parameters and relative positions of the pentagonal prism and the doublet lens are already known, the transmission matrix of the Gaussian beam M from the incident surface to the exit surface can be determined, which is

$$M = \begin{bmatrix} A & B \\ C & D \end{bmatrix} \quad (11)$$

If the parameters A, B, C and D in Eq. (11) are taken into the Eq. (10), Gaussian beam intensity of anywhere behind the doublet objective lens can be gained. When the beam is near to the axis($\theta \neq 0$) and $\Delta y = 2mm$, the light intensity distribution on the reference plane at three positions, i.e., 2mm before the focal plane, in the local plane, and 3mm behind the focal plane, is shown in Fig.28. In front of the focal plane, central line of the maximum light intensity is shifting to the positive direction of y_1 axis and behind the focal plane, it moves toward the negative direction.

As shown in the Fig.28, the intensity of the scanning laser on the focal plane is at the maximum level and the spot diameter is the smallest. When the IP has a positioning error, the intensity of the Gaussian beam decreases and the diameter of spot rapidly expands, producing a great influence on the resolution of the system. At the same time, when the intensity of the laser goes down, the amount of excited luminescence will decrease, resulting in a bad image of the IP.

Therefore, it is necessary that the manufacturing and assembling accuracy for the mechanical parts be enhanced and the installation errors be reduced in order to improve the spatial resolution of the system.

After the previous theoretical analysis and simulation calculations, Table 1 is a comprehensive presentation of the influence that various factors will have on the spatial resolution of the scanning system.
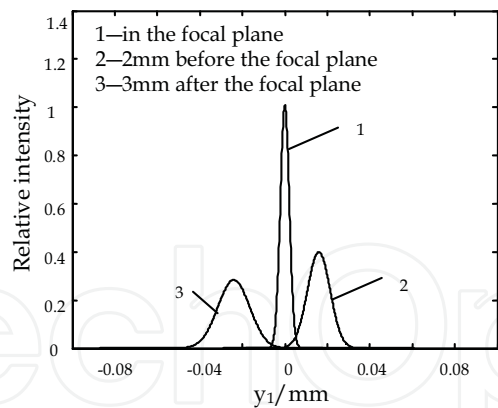
Fig. 28. Intensity distribution of different locations

	scanning arm deformation	Spherical aberration of scanning objective lens	temperature	Installation
resolution	Almost none	positive	Almost none	Huge influence

Table 1. The impact of various factors on the resolution

From Table 1, it can be seen that installation errors are the most important factors affecting the spatial resolution of a scanning system and should be given emphasis in the design, manufacturing and assembly of the laser scanning system.

4.2 An analysis of imaging stability

Since the scanning arm of the CR scanner rotates at a high speed while at work, an extra weight is needed at the opposite side of the scanning arm, which helps to keep the gravity center of the scanning sector on the motor shaft. Otherwise, if there is an offset between the gravity center and the geometric center of the scanning arm, the vibration of the scanning system will be inevitably induced, and it will make the scanning system work unstable. The model that is the equivalent of the mechanical structure when the scanning arm is rotating at a high-speed is shown Fig. 29.
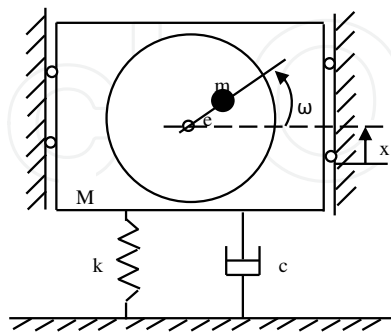

Fig. 29. Mechanical model of structure

The total mass of the rotating machinery is M, the eccentric mass of the rotor is m, the eccentricity is e, the rotation angular velocity of the rotor is ω, the base can be taken as a spring with stiffness k, and the resistance encountered in the process of vibration is simplified to the force on the mechanical structure by a damper that has been in a parallel connection with the spring and has a damping coefficient of c.

It is supposed that coordinate x represents the vertical displacement of the structure away from the equilibrium position, while the vertical displacement of the eccentric mass is $x + e\sin\omega t$, and the differential equation showing the vertical motion of the system obtained according to the D'Alembert principle is as follows

$$(M - m)\ddot{x} + m\frac{d^2}{dt^2}(x + e\sin\omega t) + c\dot{x} + kx = 0 \tag{12}$$

It can be obtained through

$$M\ddot{x} + c\dot{x} + k = me\omega^2\sin\omega t \tag{13}$$

Where me is called amount of unbalance, and $me\omega^2$ is the centrifugal force caused by amount of unbalance. The steady state response of the system is as follows

$$x(t) = B\sin(\omega t - \phi) \tag{14}$$

The amplitude of vibration of the steady state response is as follows

$$B = \frac{me}{M}\frac{\lambda^2}{\sqrt{(1 - \lambda^2)^2 + (2\xi\lambda)^2}} \tag{15}$$

The phase difference between the displacement of the vibrating object and the exciting force is as follows

$$\phi = arctg\frac{2\xi\lambda}{1 - \lambda^2} \tag{16}$$

Where $\omega_n = \sqrt{\dfrac{K}{M}}$ is the natural frequency, $\lambda = \dfrac{\omega}{\omega_n}$ is the frequency ratio, and $\xi = \dfrac{c}{2\omega_n M}$ is the damping coefficient.

It can known from Eq. (15) and Eq. (16) that when the frequency is low ($\omega << \omega_n$), the amplitude of vibration is nearly zero; when the frequency is high ($\omega >> \omega_n$), the amplitude of vibration approaches a constant of me/M that is almost unrelated to the frequency and the damping coefficient of the system; when resonance happens ($\omega = \omega_n$), the amplitude of vibration is $B = me/2\xi M$ and smaller damping coefficient will lead to greater vibration. When $\omega \approx \omega_n$, the phase difference will undergo a sudden anti-phase change of 180° and the resonance will take place.

For rotating machinery, the centrifugal force caused by the deviation of the center of gravity is one of the major motivation sources of vibration. When the frequency of motivation force, namely, the angular velocity ω of the rotor is close to the natural frequency ω_n of the system, there will be resonance in the system. The motor speed at this moment is called the critical speed.

A simplified model of the mechanical structure of the scanner through three-dimension mapping software is shown in Fig.30, and the results of the finite element analysis are shown in Fig.31. There are total of 245041 grid nodes and 72149 units after finite element model meshing. The first six natural frequencies of the system and the corresponding speed of the motor when system resonates are shown in Table 2.
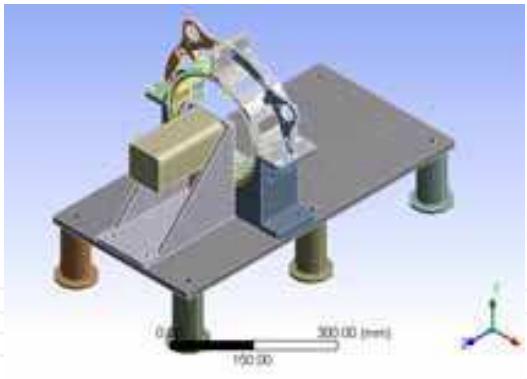
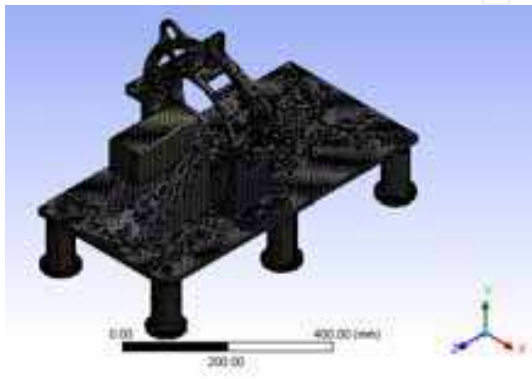Fig. 30. Mechanical structure of scanner

Fig. 31. Finite element mesh of the structure

From the Table2, it can be concluded that when the rotating parts of the scanner have the mass eccentricity, the system will vibrate, the amplitude of vibration will become large if the eccentricity increases; When the angular velocity is equal to the natural frequency of the system, the resonance will be generated, which will not only considerably deform the structure of the system and will also destabilize the system; The motor speed is associated to the systematic sampling frequency, and a high sampling frequency is needed if the motor rotates at a high speed. Therefore, after having determined the sampling frequency, the motor speed should be to calculated and also be kept away from the natural frequency of the mechanical system.

Mode order	1	2	3	4	5	6
Natural frequency(Hz)	220.58	289.68	379.33	413.63	444.51	463.75
motor rotation speed(rpm)	2106.4	2759.7	3622.3	3949.9	4244.8	4428.5

Table 2. Systematic natural frequency and related motor speed

5. Experimental results and analysis

Currently in China, the spatial resolution required in industrial radiographic testing is generally no less than 3Lp/mm. The German-made 20Lp/mm resolution testing card is applied to test this scanning system and the testing results show that the spatial resolution

of 7Lp/mm can be obtained by the developed system, which can meet the demand of China's industrial X-ray testing.

Experiments are carried out on the developed prototype in the testing of the steel pipe weld. The steel pipe used in the experiment of weld imaging has a diameter of 160 mm and its wall is 8mm thick, with the IP bent in the pipe as shown in Fig. 32. Experimental conditions include the X-ray tube voltage of 120KV, the tube current of 4mA, the focal length 700mm, the exposure time 40s. After scanning and reading with the laser scanner developed, the original image gotten by this system is as shown in Fig. 33, in which even a small weld defect can be seen clearly without any image processing.
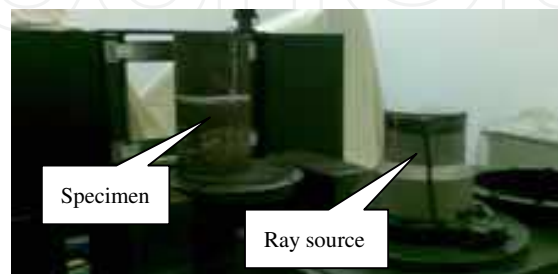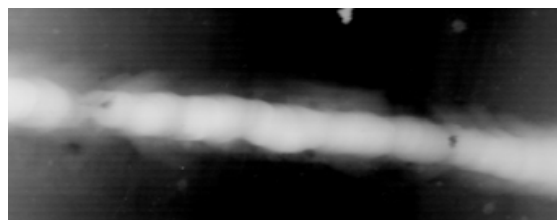

Fig. 32. The experiment of radiography

Fig. 33. Original image of scanning

6. Conclusions

A new laser scanning method and technology for the CR system is proposed here with designs accomplished for the optical system, the signal collection and control system, the mechanical system, and the software as well as the development of a CR scanner prototype; An analysis has been made on the a various factors that influence the system's spatial resolution and other performances, the results of which show that the positioning error of the IP is the key one. When the IP moves away from the focal plane of the scanning objective lens, the laser has a smaller intensity after focusing, the diameter of the spot becomes larger, and the spatial resolution decreases rapidly; the finite element simulation has been conducted on the mechanical structure to justify the effort to avoid resonance of the system. Some experiments have been carried out on the prototype that has been developed and the results of these experiments show that the quality of imaging of the scanning system developed is able to meet the demand of China's industrial X-ray imaging inspection.

Despite some of the good research results achieved during our work, much remains to be improved.

1. For the readout device that has been designed and developed, only half scanning is used to collect the luminescence. With regard to this problem, measures could be taken on the originally designed readout device to make the laser be focused on the IP from

two symmetrical directions at the same time. In this way, it amounts to the effect of having two scanning arms work together during the circular scanning of the IP, excluding the need for adding more counter weight. The scanning speed can be enhanced.

2. The prototype of the laser scanner leaves much to be desired, especially the mechanical part, including the fixing and support structure of the optical device and the transmission sector for the IP movement mechanism. The manufacturing and assembling accuracy is not so high, which causes the actual resolution to be lower than what has been designed. It is still quite necessary to further optimize and improve the mechanical structure and reduce the errors in process of the manufacturing and assembling.

7. Acknowledgments

8. References

AR Cowen; AG Davies & SM Kengyelics(2007). Advances in computed radiography systems and their physical imaging characteristics. *Clinical Radiology*, vol.62, No. 12, pp. 1132-1141, ISSN 0009-9260.

Abdul-Azeez R; Al-Rashed & Bahaa EA Saleh(1995). Decentered Gaussian beams. *Applied Optics*, Vol. 34, No.30,pp.6819-6825, ISSN 0003-6935.

Brandt et al. (1996). Light collector having optically coated acrylic substrate. *US. PAT*. NO. 5541421.

Claudio Palma(1997). Decentered Gaussian beams, ray bundles, and Bessel-Gauss beams. *Applied Optics*, Vol.36 No.6, pp.1116-1120, ISSN 0003-6935.

Chen H Q(2003).*Modern Practical Optical System*. Huazhong University of Science &Technology Press, ISBN：756092939, Wuhan

Michael Brandt (1993). The design and performance characteristics of a collector for high efficiency detection of photostimulable phosphor emissions. *Proceedings of SPIE - The International Society for Optical Engineering*, pp.289-295, ISBN 0819411302, Newport Beach CA USA, Febrary 1992, Publ by Society of Photo-Optical Instrumentation Engineers, Bellingham WA USA.

O. Dragusin et al. (2006). Characterization of a new generation of Computed Radiography system based on line scanning and phosphor needles. *Progress in Biomedical Optics and Imaging - Proceedings of SPIE*, pp.2113-2122,ISBN 0819464252, San Diego CA USA, Febrary 2006, SPIE, USA.

Satoshi Arakawa et al.(1999) Novel computed radiography system with improved image quality by detection of emissions from both sides of an imaging plate. *Proceedings of SPIE - The International Society for Optical Engineering*, pp.572-581, ISSN 0277786X, San Diego, CA, USA, Febrary 1999, SPIE, USA.

Schaetzing R et al. (2002). New high-speed scanning technique for computed radiography. *Proceedings of SPIE - The International Society for Optical Engineering*, pp.511-520, ISSN 0277786X, San Diego, CA, USA, Febrary 2002, SPIE-Int. Soc. Opt. Eng, USA.

Shan B Zh; Guo B P& Wang Sh Y(2005)Laser Scanning System of Large Field. *Shenzhen Science & Technology*, No.z1, pp2-7, ISSN 1009-5985.

Zhang J P; Feng X H & Huang L Q(2008). Design of laser scanning optical system for computed radiography. *Optics and Precision Engineering*, vol.16, No. 2, pp202-207, ISSN 1004-924x.

Zhou X L et al. (1993). The development of CR-IP system. *Chinese Journal of Medical instrumentation*, vol.17.No.2, pp63-68, ISSN 1671-7104

Laser Scanning, Theory and Applications

Edited by Prof. Chau-Chang Wang

Ever since the invention of laser by Schawlow and Townes in 1958, various innovative ideas of laser-based applications emerge very year. At the same time, scientists and engineers keep on improving laser's power density, size, and cost which patch up the gap between theories and implementations. More importantly, our everyday life is changed and influenced by lasers even though we may not be fully aware of its existence. For example, it is there in cross-continent phone calls, price tag scanning in supermarkets, pointers in the classrooms, printers in the offices, accurate metal cutting in machine shops, etc. In this volume, we focus the recent developments related to laser scanning, a very powerful technique used in features detection and measurement. We invited researchers who do fundamental works in laser scanning theories or apply the principles of laser scanning to tackle problems encountered in medicine, geodesic survey, biology and archaeology. Twenty-eight chapters contributed by authors around the world to constitute this comprehensive book.

How to reference

In order to correctly reference this scholarly work, feel free to copy and paste the following:

Qibo Feng, Meng Zheng, Shuangyun Shao and Zhan Gao (2011). A New Laser Scanning System for Computed Radiography, Laser Scanning, Theory and Applications, Prof. Chau-Chang Wang (Ed.), ISBN: 978-953-307-205-0, InTech, Available from: http://www.intechopen.com/books/laser-scanning-theory-and-applications/a-new-laser-scanning-system-for-computed-radiography

INTECH
open science | open minds